AIAA 81-0608R

Nonlinear Transonic Flutter Analysis

C. J. Borland* and D. P. Rizzetta†
Boeing Military Airplane Company, Seattle, Washington

A numerical procedure is presented for predicting the static and dynamic aeroelastic characteristics of thin, clean swept wings in transonic flow. The method is based upon the simultaneous time integration of the equations governing the coupled nonlinear fluid dynamic and structural aeroelastic system. Governing equations for the system are developed and the numerical algorithm, including the coupling procedure for their solution, is discussed. As a computational example, the flutter of a simple rectangular wing is considered. Solutions are presented for a range of Mach numbers and dynamic pressures and compared to other existing flutter analysis methods including doublet lattice, modified strip theory, and time linearization. Unlike other procedures, the method presented here is capable of predicting the nonlinear interaction between unsteady shock wave motions and the dynamic response of an elastic wing. Computed results indicate the existence of the "transonic bucket."

Nomenclature

a = $(1/c)(E+2G_S c\xi_y\phi_\eta)$
A = $M_\infty^2 k^2$
$[A]$ = matrix of elemental areas
A_i = $q_i(0)$
b = $(1/c^2)(F+G_S c^2\xi_y^2)$
B = $2M_\infty^2 k$
B_i = $\dot{q}_i(0)$
c = local section chord nondimensionalized by c_r
c_r = reference chord
cc_N = section normal force coefficient
C_p = pressure coefficient
D_ξ, D_η = finite difference operators
E = $1-M_\infty^2$
f = instantaneous surface definition
F = $-\frac{1}{2}(\gamma+1)M_\infty^2$
$\{F\}$ = vector of generalized forces
$\{F_A\}$ = aerodynamic contribution to vector of generalized forces
f_E = applied external force
F_z = external force
$\{F_E\}$ = external force contribution to vector of generalized forces
f_0 = $-(A\phi_t+B\phi_x)$
f_1 = $E\phi_x+F\phi_x^2+G\phi_y^2$
f_2 = $\phi_y+H\phi_x\phi_y$
f_3 = ϕ_z
g = initial ϕ distribution
$[g]$ = matrix of structural damping coefficients
G = $-\frac{1}{2}(\gamma-3)M_\infty^2$
$[G]$ = generalized damping matrix
h = initial ϕ_t distribution
H = $-(\gamma-1)M_\infty^2$
k = nondimensional time scaling, tc_r/t^*U_∞
$[k]$ = elemental stiffness matrix
$[K]$ = generalized stiffness matrix
k_c = reduced frequency, $\omega c_r/U_\infty$
m = mass per unit area
$[m]$ = elemental mass matrix
$[M]$ = generalized mass matrix
M_i = generalized mass of ith structural mode
M_∞ = freestream Mach number
$\{q\}$ = vector of generalized displacements
q_i = generalized displacement of ith structural mode
Q = dynamic pressure, $\frac{1}{2}\rho_\infty U_\infty^2$
S = wing surface area
t = nondimensional time, $kU_\infty t^*/c_r$
t^* = physical time
U_∞ = freestream streamwise velocity
w = aeroelastic deformation
x = physical streamwise coordinate nondimensionalized by c_r
x^* = physical streamwise coordinate
X = $G_N(\xi_y\phi_\xi+\phi_\eta)^2+H\xi_y^2\phi_\xi^2+H\xi_y\phi_\xi\phi_\eta+c\xi_y\phi_\eta+c\xi_y^2\phi_\xi$
y = spanwise coordinate nondimensionalized by c_r
y^* = physical spanwise coordinate
Y = $H\xi_y\phi_\xi^2+H\phi_\xi\phi_\eta+c\xi_y\phi_\xi$
z = normal coordinate nondimensionalized by c_r
z^* = physical normal coordinate
Z_i = generalized force of ith structural mode
γ = specific heat ratio
$\delta_\xi, \delta_\eta, \delta_{\xi\xi}$ = finite difference operators
Δ = finite difference
ΔC_p = $C_p^- - C_p^+$
ζ = nondimensional transformed normal coordinate
η = nondimensional transformed spanwise coordinate
ξ = nondimensional transformed streamwise coordinate
ρ_∞ = freestream density
ϕ = nondimensional perturbation velocity potential function
Φ = physical velocity potential function
Φ_i = displacement of ith structural mode
$[\Phi_A]$ = matrix of modal displacements at aerodynamic control points
$[\Phi_A']$ = matrix of modal streamwise slopes at aerodynamic control points
$[\Phi_E]$ = matrix of modal displacements at external force application points
$[\Phi_s]$ = matrix of modal displacements at structural grid points
ω = characteristic circular frequency
$[\omega^2 M]$ = diagonal matrix whose elements are $\omega_i^2 M_i$

Subscripts

A = aerodynamic
E = elastic
F = flexible
i = ith mode

Presented as Paper 81-0608 at the AIAA Dynamic Specialist Conference, Atlanta, Ga., April 9-10, 1981; submitted Oct. 1, 1981; revision received Feb. 26, 1982.

*Principal Engineer. Associate Fellow AIAA.
†Senior Specialist Engineer. Member AIAA.

le = leading edge
min = minimum value
N = normal direction
R = rigid
S = streamwise
St = steady
te = trailing edge
tip = wing tip
Un = unsteady
x,y,z,t, ξ,ζ,ξ = partial derivatives

Superscripts

n = time level
T = transposed matrix
$+$ = upper surface
$-$ = lower surface
$(\leftarrow)$ = backward difference
$(\tilde{}), (\approx)$ = intermediate values
$(\dot{})$ = derivative with respect to physical time t^*

I. Introduction

SOME of the most difficult and most dangerous problems in aircraft aeroelasticity arise in the transonic flight regime. The difficulty stems from the fact that the equations governing transonic flow are inherently nonlinear, which has effectively precluded analytical or numerical solution by traditional approaches. The danger arises because the transonic regime is often the most critical from a structural dynamic viewpoint. This has led to a situation in which new designs can only be proven adequate by extensive high-cost transonic wind tunnel testing of dynamically scaled models and by incorporation of large safety margins in certification procedures. Wind tunnel testing can, at best, provide only a limited simulation of the actual aircraft's behavior in free flight, due to both structural and fluid dynamic limitations of scale models and to the severe wall interference effects present in transonic testing. The actual extent of the safety margins present in the design, such as the traditional flutter speed margin of 20% over design dive speed, cannot be demonstrated in flight test because of either safety or performance limitations. It is essential, therefore, that accurate analysis methods, supported and verified by carefully conducted experimental procedures, form the cornerstone of the structural dynamicist's contribution to the process of designing transonic aircraft.

The search for accurate transonic flow analysis methods has occupied many researchers over a period of more than 30 years. These methods are essential to aerodynamic design and performance prediction, as well as for structural design and structural dynamic analysis. Until the 1970's, work concentrated almost exclusively on extensions of linearized theory for certain restricted applications. In 1970, Murman and Cole[1] presented work demonstrating for the first time that the essential feature of transonic flow—the presence of a mixed subsonic-supersonic flow region containing embedded shock waves—could be obtained by a simple numerical finite-difference solution of the steady two-dimensional transonic small disturbance equation. Although both steady and unsteady solutions of the Euler equations were obtained by Magnus and Yoshihara,[2,3] the computing time was considered to be prohibitive for practical computations. The work of Murman and Cole was later extended to three-dimensional steady flow over thin wings by Ballhaus and Bailey[4] and others[5,6] to include bodies, nacelles, pylons, and winglets. Steady full-potential three-dimensional methods have also become available.[7,8]

Development of methods for unsteady transonic flow has followed two distinct approaches, both of which extend the work of Murman and Cole. These are classified as "frequency-expansion" or "time-linearized" methods[9-13] and nonlinear "time-integration" methods.[14] The frequency expansion method assumes the unsteady flowfield to be a linear harmonic perturbation about a mean steady state. The resulting linear unsteady equation may be solved by relaxation or by time integration for motion at a given frequency. Since the mean location of shock waves in the frequency expansion method is given by the steady-state solution, shock motions are constrained to be small motions about the steady location. The assumption of a linear perturbation may be adequate under certain circumstances, and is certainly convenient if traditional linearized aeroelastic stability analysis procedures are to be used. However, it may be a dangerous one to make a priori since the potentially important nonlinear effects of large amplitude shock motions, harmonic interaction, and amplitude sensitivity will be missing from the results. Indeed, there is considerable evidence, both analytical[14,15] and experimental[16] that unsteady transonic flows do not exhibit the behavior of this simple linear perturbation model. Furthermore, it is unclear that these linearized methods could be effectively applied when a large number of vibration modes and a considerable frequency range must be encompassed, since a separate computation would be required for each mode and each frequency combination. Also, until recently[17] such methods have been restricted by numerical difficulties to very low-frequency motions.

The alternate approach of time integration removes many of the limitations of the frequency expansion method. Most importantly, since a time-dependent nonlinear equation is solved, the motion (including the disappearance) of shock waves can be accurately predicted. Ballhaus and Goorjian[14] demonstrated the ability of the method to reproduce various types of irregular (periodic but nonsinusoidal) shock motions that have been observed experimentally. From an aeroelastic viewpoint, there has been considerable discussion recently[18] about the importance of shock motion in transonic aeroelastic stability (flutter), thus evidencing an urgent need for a method that accurately accounts for these effects. Additional attractive features of the time-integration method are the ability to handle general unsteady (rather than sinusoidal) motion, the incorporation of nonlinear effects of finite motion amplitude, and the removal of frequency limitations, provided that the proper time-dependent terms are included in the formulation.[19] For aeroelastic calculations, it is possible to couple the aerodynamic and structural equations directly, rather than using the indirect approach of calculating aerodynamic forces for each structural mode and frequency combination independently. This was the first demonstrated for a single degree-of-freedom pitching oscillation,[20] and later for simple two-dimensional aeroelastic systems.[21-23] The methodology for providing the coupling with three-dimensional aeroelastic systems, employing an arbitrary number of degrees of freedom, is presented here.

An extension of the two-dimensional time-integration method of Ballhaus and Goorjian[14] to three-dimensional unsteady transonic flow about swept wings was considered by Borland et al.[24] Details of the governing equations, coordinate transformation, and numerical algorithm necessary for solution of the low-frequency approximation to the modified[25] three-dimensional unsteady transonic small disturbance equation may be found in Ref. 24. The extension of this method to incorporate high-frequency effects in the differential equation and boundary conditions, and coupling of the method with the solution of equations for static and dynamic aeroelastic problems are described herein.

II. Formulation of the Aerodynamic Problem

It is assumed that the fluid motion may be described by the modified three-dimensional transonic small disturbance equation for unsteady inviscid flow in the form

$$\frac{\partial f_0}{\partial t} + \frac{\partial f_1}{\partial x} + \frac{\partial f_2}{\partial y} + \frac{\partial f_3}{\partial z} = 0 \tag{1}$$

where

$$f_0 = -(A\phi_t + B\phi_x) \tag{2a}$$

$$f_1 = E\phi_x + F\phi_x^2 + G\phi_y^2 \tag{2b}$$

$$f_2 = \phi_y + H\phi_x\phi_y \tag{2c}$$

$$f_3 = \phi_z \tag{2d}$$

Here, ϕ is the perturbation velocity, potential function defined from the complete potential Φ as

$$\Phi(x^*,y^*,z^*,t^*) = U_\infty c_r[x + \phi(x,y,z,t)] \tag{3}$$

where the physical dimensions x^*, y^*, z^*, t^* have been nondimensionalized as

$$x = x^*/c_r \quad y = y^*/c_r \quad z = z^*/c_r \quad t = kU_\infty t^*/c_r \tag{4}$$

In Eq. (4) c_r is the chosen reference length (usually the root chord) and k is a nondimensional scaling factor on time. Also,

$$A = M_\infty^2 k^2 \quad B = 2M_\infty^2 k \quad E = 1 - M_\infty^2 \quad F = -\tfrac{1}{2}(\gamma+1)M_\infty^2$$
$$G = \tfrac{1}{2}(\gamma-3)M_\infty^2 \quad H = -(\gamma-1)M_\infty^2 \tag{5}$$

A steady three-dimensional equation analogous to Eq. (1) was proposed by Lomax et al.,[25] where it was pointed out that the nonlinear cross terms proportional to G and H were necessary for the proper capture of swept shocks on wings with sweep angle greater than about 15 deg. Unlike the "classical" equation where $G = H = 0$, the specific form of the cross terms used here cannot be obtained by any formal limiting process. Experience with steady-state, three-dimensional solutions, however, has shown their inclusion to be necessary for the accurate reproduction of experimental results.[26] Alternate forms of the coefficients F, G, and H are also possible.[27]

Boundary Conditions

The boundary conditions for the flowfield and wing surface may be stated as

$$\phi = 0 \qquad \text{(far upstream)} \tag{6a}$$

$$\phi_x + k\phi_t = 0 \qquad \text{(far downstream)} \tag{6b}$$

$$\phi_z = 0 \qquad \text{(far above and below)} \tag{6c}$$

$$\phi_y = 0 \qquad \text{(far spanwise)} \tag{6d}$$

$$\phi_y = 0 \qquad \text{(wing root)} \tag{6e}$$

On the wing surface defined by $z = f^{\pm}(x,y,t)$, the linearized unsteady boundary condition

$$\phi_z^{\pm} = f_x^{\pm} + kf_t^{\pm} \tag{7a}$$

is applied on

$$z = 0^{\pm} \qquad x_{le} \le x \le x_{te} \qquad y \le y_{tip} \tag{7b}$$

Across the trailing vortex sheet in the wake given by $z = 0$ for $x > x_{te}$ the contact surface conditions

$$[\phi_z] = 0 \qquad \text{(continuity of slope)} \tag{8a}$$

and

$$[\phi_x + k\phi_t] = 0 \qquad \text{(continuity of pressure)} \tag{8b}$$

are applied, where the brackets denote the jump in the enclosed quantity across the vortex sheet. Finally, the problem is fully defined by specification of the initial conditions

$$\phi(x,y,z,0) = g(x,y,z) \qquad \phi_t(x,y,z,0) = h(x,y,z) \tag{9}$$

The above boundary conditions are applied if a "free-flight" computation is being performed. Conditions (6c) and (6d) are the equivalent of assuming solid walls at a large distance from the wing and have proven effective in previous methods.[4,14] Some improvements in computational efficiency or accuracy can probably be achieved by considering the computational boundaries closer to the wing and using "nonreflecting" far-field boundary conditions.[28] Alternate flowfield boundary conditions[29] can be applied in the case of ventilated wind tunnel walls.

The structural surface boundary condition, represented by Eq. (7) and appropriate for a small disturbance method, is a simple one: flow tangency at the wing surface satisfied on the mean chord plane. In Eq. (7) $f^{\pm}$ represents the local time-dependent description of the upper (+) and lower (−) surface ordinates. This description can be used to incorporate geometric shape, rigid motion, and static and dynamic aeroelastic effects.

For a steady-state calculation on a rigid wing, the local surface velocities $f_t^{\pm}$ are zero and the local surface slopes $f_x^{\pm}$ are given by the superposition of geometric angle of attack, local twist, and slope due to airfoil section geometry. Additional complexities arise in the cases of specified unsteady motion, static aeroelastic deflection, dynamic aeroelastic motion, control surface deflection, or atmospheric gusts.

Transformation of Coordinates

For purposes of computational convenience, the following shearing transformation is applied in order to map a swept tapered wing planform in the physical domain into a rectangular planform in the computational domain. We define

$$\xi = \frac{x - x_{le}}{c} \qquad \eta = y \qquad \zeta = z \tag{10}$$

where c is the local chord nondimensionalized by c_r. This transformation leads to a final form of the equation to be solved numerically:

$$cA\phi_{tt} + B\phi_{\xi t} = \frac{\partial}{\partial\xi}(a\phi_\xi + b\phi_\xi^2) + 2G_S\phi_\eta\phi_{\xi\eta}$$
$$+ \frac{\partial}{\partial\eta}(c\phi_\eta) + c\frac{\partial^2\phi}{\partial\zeta^2} + \frac{\partial X}{\partial\xi} + \frac{\partial Y}{\partial\eta} \tag{11}$$

where

$$a = (1/c)(E + 2G_S c\xi_y\phi_\eta) \tag{12a}$$

$$b = (1/c^2)(F + G_S c^2\xi_y^2) \tag{12b}$$

$$X = G_N(\xi_y\phi_\xi + \phi_\eta)^2 + H\xi_y^2\phi_\xi^2 + H\xi_y\phi_\xi\phi_\eta + c\xi_y\phi_\eta + c\xi_y^2\phi_\xi \tag{12c}$$

$$Y = H\xi_y\phi_\xi^2 + H\phi_\xi\phi_\eta + c\xi_y\phi_\xi \tag{12d}$$

and G_S, G_N represent a splitting of the coefficient G in Eq. (2b) into streamwise and normal contributions, such that $G_S = 1 - M_\infty^2$.

Numerical Algorithm

The time-accurate solution of Eq. (11) may be obtained by the following first-order (Δt) accurate approximate fac-

torization alternating direction implicit (ADI) algorithm:

ξ sweep:

$$B\bar{\delta}_\xi\left(\frac{\tilde{\phi}-\phi^n}{\Delta t}\right)=D_\xi\left[a^n\left(\frac{\tilde{\phi}_\xi+\phi^n_\xi}{2}\right)+b\phi^n_\xi\tilde{\phi}_\xi\right]$$
$$+2G_S(\delta_\eta\phi^n)D_\eta(\bar{\delta}_\xi\phi^n)+\delta_\eta(c\delta_\eta\phi^n)$$
$$+c\delta_{\zeta\zeta}\phi^n+\delta_\xi X^n+\delta_\eta Y^n \tag{13a}$$

η sweep:

$$B\bar{\delta}_\xi\left(\frac{\tilde{\tilde{\phi}}-\tilde{\phi}}{\Delta t}\right)=\frac{1}{2}\delta_\eta(c\delta_\eta\tilde{\tilde{\phi}}-c\delta_\eta\phi^n)$$
$$+G_S(\delta_\eta\phi^n)D_\eta(\bar{\delta}_\xi\tilde{\tilde{\phi}}-\bar{\delta}_\xi\phi^n) \tag{13b}$$

ζ sweep:

$$cA\left(\frac{\phi^{n+1}-2\phi^n+\phi^{n-1}}{\Delta t^2}\right)+B\bar{\delta}_\xi\left(\frac{\phi^{n+1}-\tilde{\tilde{\phi}}}{\Delta t}\right)$$
$$=\frac{c}{2}\delta_{\zeta\zeta}(\phi^{n+1}-\phi^n) \tag{13c}$$

where δ_ξ, δ_η, $\delta_{\zeta\zeta}$ are second-order accurate central-difference operators, $\bar{\delta}_\xi$ is a first-order backward-difference operator, and D_ξ, D_η are mixed type-dependent difference operators. The details of the numerical method represented by Eq. (13) are summarized in Ref. 24 and discussed in full detail in Ref. 30. The difference between the present description and that of Ref. 24 arises in the incorporation of the term representing the second derivative of velocity potential with respect to time (ϕ_{tt}) in the third sweep and the incorporation of time-derivative terms in the wake, the downstream boundary conditions, and the calculation of pressure coefficients. Inclusion of these terms is necessary to account for "high-frequency" effects, that is, flows with a reduced frequency k_c greater than about 0.4, where $k_c=\omega c_r/U_\infty$ represents the ratio between the time scales of the moving fluid and surface motion at some characteristic circular frequency ω. Numerical stability of the original algorithm appears to be slightly improved by the addition of the ϕ_{tt} term.

The numerical algorithm represented by Eq. (13) is used to advance the velocity potential in the computational domain from time step n to time step $n+1$. It is applied repeatedly until some previously established condition (such as convergence of a steady flowfield or completion of a specific number of time steps) is fulfilled.

Aerodynamic Pressures and Coefficients

Once the perturbation potential ϕ is obtained by the solution of Eq. (11), the local pressure coefficient on the upper and lower surfaces is obtained as

$$C_p^{\pm}=-(2/c)\phi_\xi^{\pm}-2k\phi_t^{\pm} \tag{14}$$

and the total aerodynamic force and moment coefficients are found by integration of the pressure differential. For example, the spanwise distribution of normal force is given by

$$cc_N(y)=c\int_0^1\Delta C_p\,d\xi \tag{15}$$

where

$$\Delta C_p=C_p^--C_p^+ \tag{16}$$

Other coefficients may be obtained in a similar manner.

III. Formulation of the Aeroelastic Problem

The general nature of the aeroelastic problem involves the balance between the aerodynamic forces on a vehicle, the structural forces created by elastic deformations, and the inertial forces. This is true whether the problem is one of static equilibrium, dynamic aeroelastic stability, or dynamic response. In this section, the method previously described for calculation of the steady and unsteady aerodynamic forces on thin wings in transonic flow will be coupled with structural equations of motion to form a unified aeroelastic method.

Structural Equations of Motion

A convenient and economical representation of the static and dynamic characteristics of a flexible airplane structure is the concept of generalized coordinates.[31] In this concept, the physical deformations of an elastic structure are represented by a generalized coordinate transformation, where the generalized coordinates are given by calculated or assumed modes of the structure. A common representation, and one usually leading to the most accurate representation of structural deformation with the smallest number of generalized coordinates, employs orthogonal free-vibration mode shapes. Here the time-dependent deformation of a thin restrained wing subject to a time-varying force is given by the infinite series

$$w(x^*,y,^*t^*)=\sum_{i=1}^{\infty}\Phi_i(x^*,y^*)q_i(t^*) \tag{17}$$

where $\Phi_i(x^*,y^*)$ is the displacement of the structure in the ith free-vibration mode. The generalized displacement $q_i(t^*)$ specifies the amount of the ith mode participating in the deformed shape, and is given by solution of the following ordinary-differential equation:

$$M_i\ddot{q}_i+M_i\omega_i^2q_i=Z_i \qquad (i=1,2,\ldots,\infty) \tag{18}$$

where

$$M_i=\int\int_S\Phi_i^2(x^*,y^*)m(x^*,y^*)dx^*dy^* \tag{19}$$

is known as the generalized mass of the ith mode and

$$Z_i(t^*)=\int\int_S F_z(x^*,y^*,t^*)\Phi_i(x^*,y^*)dx^*dy^* \tag{20}$$

is the time-dependent generalized force in the ith vibration mode of natural frequency ω_i. In the above equation, $m(x^*,y^*)$ represents the mass per unit area and $F_z(x^*,y^*,t^*)$ the applied time-dependent external force per unit area. The integrals are carried out over the wing surface area S. To complete the problem, $q_i(0)=A_i$ and $\dot{q}_i(0)=B_i$ are prescribed as initial conditions on displacement and velocity for each of the generalized displacements.

The time-dependent external force may be composed of motion-dependent aerodynamic forces and applied external forces

$$F_z(x^*,y^*,t^*)=\tfrac{1}{2}\rho_\infty U_\infty^2\Delta C_p(x^*,y^*,t^*)+f_E(x^*,y^*,t^*) \tag{21}$$

where $\frac{1}{2}\rho_\infty U_\infty^2$ is the freestream dynamic pressure, $\Delta C_p(x^*,y^*,t^*)$ the time-dependent aerodynamic load distribution, and $f_E(x^*,y^*,t^*)$ an applied external force. It may be noted that physical independent variables have been used here, as is customary in aeroelastic formulations.[32]

The system of Eqs. (17-21) represents an exact formulation of the problem if an infinite number of orthogonal modal coordinates is used. In actual practice, only a finite number of modes is usually available from a lumped-parameter solution of the free-vibration problem. The number of modes available

is equal to the number of dynamic degrees of freedom in the vibration analysis. A further reduction in this set, known as "modal truncation"[33] is usually employed in structural dynamic analysis. The number of modes necessary to represent the deformations of the system is problem dependent, ranging from two or three for simple beams to a few dozen for complex aircraft structures. Although many variations of the method, such as the method of residual flexibility,[33] have appeared in the literature over the years, the basic form has been adopted herein for simplicity. With a finite number of mode shapes, the following matrix formulation of Eq. (18) can be conveniently adopted.

$$[M]\{\ddot{q}\} + [K]\{q\} = \{F\} \tag{22}$$

where

$$[M] = [\Phi_s]^T[m][\Phi_s] \tag{23}$$

and

$$[K] = [\sim\omega^2 M\sim] = [\Phi_s]^T[k][\Phi_s] \tag{24}$$

where $[m]$ and $[k]$ represent the elemental mass and stiffness matrices arising from the lumped-parameter structural idealization, and $[\Phi_s]$ represents the displacement of the natural vibration modes at a chosen set of structural grid points. The generalized forces can be written as

$$\{F\} = \{F_A\} + \{F_E\} = \tfrac{1}{2}\rho_\infty U_\infty^2[\Phi_A]^T[A]\{\Delta C_p\} + [\Phi_E]^T\{f_E\} \tag{25}$$

where $[A]$ represents the diagonal matrix of elemental areas assigned to each of the aerodynamic control points, $\{\Delta C_p\}$ is the lifting pressure at each of these control points, $\{f_E\}$ the applied external force, and $[\Phi_A]$ and $[\Phi_E]$ the modal displacements at the aerodynamic and external force application control points.

Equation (22) is a valid representation of the structural dynamics of a flexible wing if the structural system is conservative. In an actual structure, dissipative forces are present in the form of material damping in metals and adhesives, free play in joints and fasteners, effects of nonstructural elements, etc. These are extremely difficult to estimate analytically, and may be incorporated into the model as a "structural damping coefficient" on each free-vibration mode (based on experimental data, previous experience, or an ad hoc assumption) with the damping specified as a velocity-dependent force. Thus, Eq. (22) is rewritten as

$$[M]\{\ddot{q}\} + [G]\{\dot{q}\} + [K]\{q\} = \{F\} \tag{26}$$

where

$$[G] = [\sim g\sim][K]^{1/2}[M]^{1/2} \tag{27}$$

and g_i is the specified structural damping coefficient for each natural mode. In the above development, the structural damping is treated as an equivalent viscous damping[34] and differs from the usual "artificial" damping of the V-g flutter solution method[35] in that the g_i's are treated as known quantities, estimated or measured, rather than as unknown parameters determined as part of the solution.

Boundary Conditions for Aeroelastic Coupling

The solution to the system of structural equations of motion is coupled to the aerodynamic solution through the boundary conditions. The flowfield boundary conditions, as specified in Eq. (6), remain unchanged for the aeroelastic problem. The structural surface boundary condition, Eq. (7), may now be considered to contain terms that are specified and terms that are determined by solution to the aeroelastic equations. Because of the nonlinear nature of the aerodynamic problem, and the assumed linear nature of the structural response, the appropriate method of determining the actual unsteady pressure distribution, integrated forces, and associated structural response may be summarized as:

1) Determine the actual time-dependent deformed shape and motion as the sum of contributions from the static rigid, static flexible, dynamic rigid, and dynamic flexible components.

2) Calculate the pressure distribution and integrated generalized forces on this actual deformed shape in a time-dependent fashion.

3) Apply these forces through the structural equations of motion to determine response.

This is significantly different from the usual linearized method of aeroelastic analysis, which consists of the following procedure:

1) The pressure distribution for each modal component of the deformed aircraft shape and motion (for example, rigid body and structural modes) are calculated separately and integrated to give generalized forces.

2) The resulting forces are summed linearly in the solution of the equations of motion to determine response.

3) If the forces are considered to be those due to harmonic motion, the process is repeated for each of a set of frequencies in the range of interest.

The structural surface boundary conditions on the velocity potential for static aeroelastic analysis are as follows:

$$\{\phi_z^{\pm}\} = \{f_{x_R}^{\pm}\} + \{f_{x_F}\}; \quad \begin{cases} x_{le} \le x \le x_{te} \\ y \le y_{tip} \end{cases} \tag{28}$$

where the rigid component f_{x_R} can contain contributions from the local slope of the airfoil section coordinate definition of the upper and lower surface, the geometric angle of attack, the static rigid twist distribution (jig twist), and static control surface deflections.

The flexible component f_{x_F}, which is considered to be the same for the upper and lower surface, may be defined as

$$\{f_{x_F}\} = [\Phi_A']\{q\} \tag{29}$$

where $[\Phi_A']$ is the matrix of streamwise slopes of the natural or assumed vibration modes defined at the aerodynamic control points, and $\{q\}$ is the matrix of static values of the generalized displacements. (Determination of these values is described in the following section.) For dynamic aeroelastic analysis, the structural surface boundary conditions may be written as a combination of steady and unsteady terms:

$$\{\phi_z^{\pm}\} = \{f_{x_R}^{\pm}\}_{St} + \{(f_x^{\pm} + kf_t^{\pm})_R\}_{Un} + \{(f_x^{\pm} + kf_t^{\pm})_F\}_{Un} \tag{30}$$

The first term is identical to the corresponding term for static aeroelastic analysis containing contributions of airfoil slope, static angle of attack, static twist, and static control deflection. The second, or "rigid unsteady" term contains contributions from prescribed rigid body motions (i.e., pitch and plunge), control surface motions, and can even include the time and space-varying downwash contribution of a vertical gust. The third, or "flexible unsteady" term is the contribution from time-varying deformation of the flexible structure defined as:

$$\{(f_x + kf_t)_F\}_{Un} = [\Phi_A']\{q\} + \frac{l}{U_\infty}[\Phi_A]\{\dot{q}\} \tag{31}$$

The time dependence of the generalized displacements may be prescribed (such as sinusoidal or indicial motion) or may be determined by solution of the equations of motion, Eq. (26).

IV. Aeroelastic Solution Procedure

Static Aeroelastic Solution

Solution for the static deformed shape, flexible aerodynamic coefficients, and static aeroelastic loads may be accomplished by an iterative solution of Eq. (26) for the case when velocities and accelerations are considered to be zero, that is, by solution of

$$[K]\{q\} = \{F\} \tag{32}$$

This may be readily accomplished by use of inversion or any of several linear equation solution routines, provided that the generalized stiffness matrix $[K]$ is not singular. Since for orthogonal modes the matrix is diagonal and the elements are related to the generalized masses by the modal natural frequencies [Eq. (24)], this condition implies that rigid body (zero-frequency) modes cannot be included in the static aeroelastic solution set of modes. Static trim cannot be determined directly, therefore, but must be found iteratively by specifying aircraft angle of attack and/or control deflections, determining the resultant total lift and moment, and resetting angle of attack, etc.

Once the static solution for generalized displacements is determined, the new boundary conditions [Eq. (29)] are applied, the flowfield is recomputed, and the process is repeated to convergence. Initial studies have shown that for the cases considered, static aeroelastic solutions can be obtained with essentially the same amount of computational effort as static rigid solutions or with very few additional cycles on a previously calculated static rigid solution.

Dynamic Aeroelastic Solution

Solution of the dynamic aeroelastic problem involves time-domain integration of the set of simultaneous ordinary-differential equations, Eq. (26), in which the nonhomogeneous part is determined at each time step as part of the solution. There is a large variety of computational methods for accomplishing this with various properties of stability, convergence, accuracy, and efficiency. The approach followed in this study was to assume that a simple integration technique, applied at each aerodynamic computational step, would be adequate, since 1) the computation effort is dominated by the finite-difference solution of the nonlinear flow equations, and 2) a simple method would provide an accurate solution if the time step were small enough. These assumptions were checked by comparison of computing times for dynamic rigid and dynamic flexible problems, and by integrating the homogeneous equations of motion. The natural vibration frequencies and displacements were recovered accurately for all modes in the test problem chosen.

The method of solving Eq. (26) is the same as that used in Ref. 23 for the problem of transonic aileron buzz where a simple centered difference in time was used.

Thus,

$$\{\ddot{q}\} = \left\{\frac{q^{n+1} - 2q^n + q^{n-1}}{(\Delta t^*)^2}\right\} \tag{33a}$$

and

$$\{\dot{q}\} = \left\{\frac{q^{n+1} - q^{n-1}}{2\Delta t^*}\right\} \tag{33b}$$

Substituting into the set of equations of motion leads to a simple implicit solution for the generalized displacements at step $n+1$ as a function of the forces and displacements at steps n and $n-1$:

$$\{q^{n+1}\} = \left[\left(\frac{1}{\Delta t^*}\right)^2 M + \left(\frac{1}{2\Delta t^*}\right)G\right]^{-1}\{F^n\} + \left[\left(\frac{1}{\Delta t^*}\right)^2 M + \left(\frac{1}{2\Delta t^*}\right)G\right]^{-1}\left[2\left(\frac{1}{\Delta t^*}\right)^2 M - K\right]\{q^n\} + \left[\left(\frac{1}{\Delta t^*}\right)^2 M + \left(\frac{1}{2\Delta t^*}\right)G\right]^{-1}\left[\left(\frac{1}{2\Delta t^*}\right)G - \left(\frac{1}{\Delta t^*}\right)^2 M\right]\{q^{n-1}\} \tag{34}$$

Specification of initial conditions (e.g., generalized velocity and displacement at the beginning of the dynamic solution) is required.

The time-dependent solutions of generalized displacements can be examined to determine aeroelastic stability, and superimposed as in Eq. (17) to determine aeroelastic deformations. Dynamic aeroelastic load distributions can be determined by integration of the time-dependent surface pressures.

V. Aeroelastic Example and Results

The unified aeroelastic method described above has been incorporated in a computer code known as XTRAN3S.[36,37] All of the results presented here were computed on a nonuniform $60 \times 20 \times 40$ (ξ, η, ζ) computational mesh with the wing surface defined by 39×16 of these points in the ξ-η plane. The minimum grid spacing and computational boundaries are given as:

$$\Delta\xi_{\min} = 0.01 \qquad -15.375 \le \xi \le 26.575$$

$$\Delta\eta_{\min} = 0.05 \qquad 0.0 \le \eta \le 5.0 \quad (\eta_{\text{tip}} = 3.33)$$

$$\Delta\zeta_{\min} = 0.025 \qquad -13.0375 \le \zeta \le 13.0375$$

With this mesh, approximately 4 s of CPU time (CDC 7600) were required for each coupled fluid dynamic-aeroelastic solution time step. A typical static aeroelastic solution can be performed in about 300-400 steps, and a dynamic aeroelastic solution can be performed in about 1000 steps with $\Delta t = 0.1$. The number of steps required are case dependent, however, with complicated dependencies on planfom, airfoil section, Mach number, and frequency range of the aeroelastic modes.

The method employed for calculating flutter solutions using the coupled aeroelastic method may be summarized as follows.

1) For a particular Mach number and corresponding angle of attack, calculate the "static rigid" solution using the aerodynamic method described above, and save the resulting steady flowfield to restart the dynamic solution.

2) For a particular flight condition, choose the dynamic pressure corresponding to the chosen altitude and Mach number.

3) The initial conditions for dynamic integration of the generalized displacements may either be chosen explicitly or calculated by the "static aeroelastic" procedure employed in the program.

4) The "dynamic aeroelastic" procedure is started and run for a specified number of steps. The damping and frequency in each of the aeroelastic coupled-mode responses can be extracted from the calculated time histories of the generalized displacements.

5) The "flutter point," that is, the condition where one of the generalized displacements exhibits neutrally damped behavior, can then be determined by interpolation of the results for solutions run at several different dynamic pressures.

In order to demonstrate the application of the method to an aeroelastic problem, the flutter of a simple constant-section rectangular wing of moderate aspect ratio in transonic flow has been computed. Figure 1 shows the planform and aerodynamic parameters of the wing. A uniform cantilever beam is used as the structural model. Structural parameters, calculated natural frequencies, and modal descriptions are given in Ref. 38. This example was previously used in Ref. 38 to compare the results of the time-linearized transonic method of Ref. 12 with flutter results calculated using the doublet-lattice method and unmodified strip theory with a Prandtl-Glauert compressibility correction. In that analysis, two uncoupled assumed bending and torsion modes were used, while for the present study six cantilever coupled modes were calculated and interpolated to the aerodynamic control points.

It should be noted that each dynamic aeroelastic solution in the time domain is a so-called "matched-point" solution if the dynamic pressure, freestream velocity, and Mach number are chosen consistently with standard atmospheric parameters. A matched-point solution requires that the assumed Mach number and density correspond to the resultant flutter velocity. For traditional methods employing frequency domain solutions, an iterative procedure, such as that of Ref. 39, is usually required. In the examples shown in Ref. 38, no attempt was made to obtain matched-point solutions. In the results presented here, the velocity was selected to be consistent with that analysis rather than with a standard atmosphere.

Figure 2 shows a summary of the results of several types of transonic flutter analysis, including the linearized doublet lattice method,[40] modified strip theory,[41] the time-linearized frequency expansion transonic method,[12,38] and the full nonlinear transonic method described above. In the modified strip theory results, section lift curve slope and section centers of pressure were obtained using the "static rigid" procedure of XTRAN3S. This simulated the incorporation of empirical corrections obtained from static wind tunnel tests.

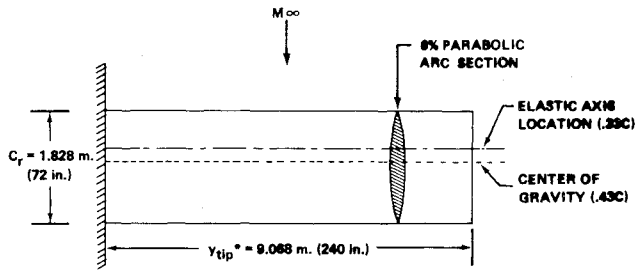

Fig. 1 Demonstration case for nonlinear transonic flutter analysis.

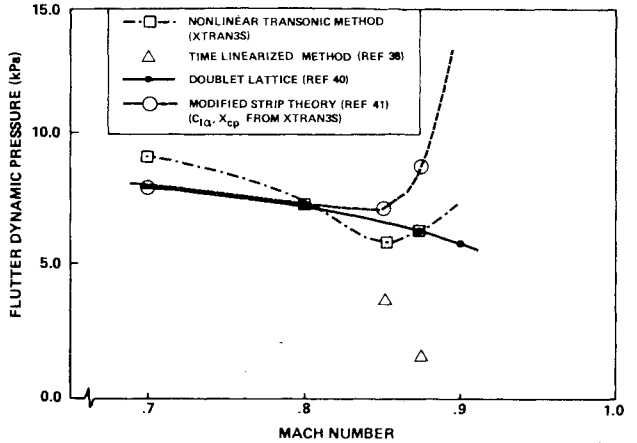

Fig. 2 Summary of flutter results for rectangular wing.

Nonlinear transonic flutter analysis of the rectangular wing was conducted at Mach numbers 0.80, 0.85, and 0.875. It may be seen that the "transonic bucket" is predicted by the nonlinear method of approximately the same Mach number as by modified strip theory (using static corrections from a nonlinear transonic calculation), but predicted flutter dynamic pressures are lower at the most critical Mach number. This may be an indication of the importance of "phasing" between motion and resultant aerodynamic forcing, as this is one fundamental difference between the full nonlinear unsteady transonic method and the modified strip method. The time-linearized method of Ref. 12 predicts considerably lower flutter dynamic pressure for the two Mach numbers calculated in Ref. 38. No transonic bucket is predicted by the uncorrected linearized doublet lattice method. The reduced frequency at flutter is about 0.1 (based on semichord) for all the flutter points obtained.

Results of the nonlinear transonic method for Mach number 0.875, which may be considered as typical, are shown in Figs. 3-6. A deflection of 1.0 in the first generalized displacement [corresponding to a 2.54 cm (1 in.) deflection at the outboard end of the elastic axis in the first coupled cantilevered mode] was specified as the initial condition. The simultaneous solution of the coupled unsteady transonic and elastic equations of motion was then allowed to proceed with three different levels of freestream dynamic pressure specified—5.21, 8.68, and 12.15 kPa (0.75, 1.25, 1.75 lb/in.^{2}). The resultant time histories of the generalized displacement of the first mode are shown in Fig. 3.

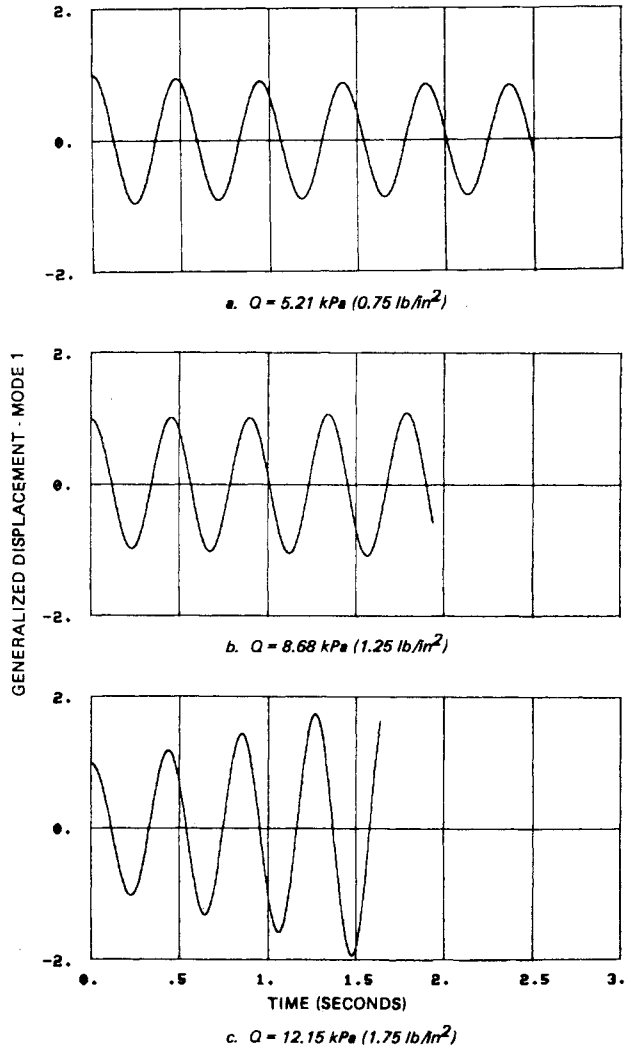

Fig. 3 Time history of first generalized displacement at $M_\infty = 0.875$.

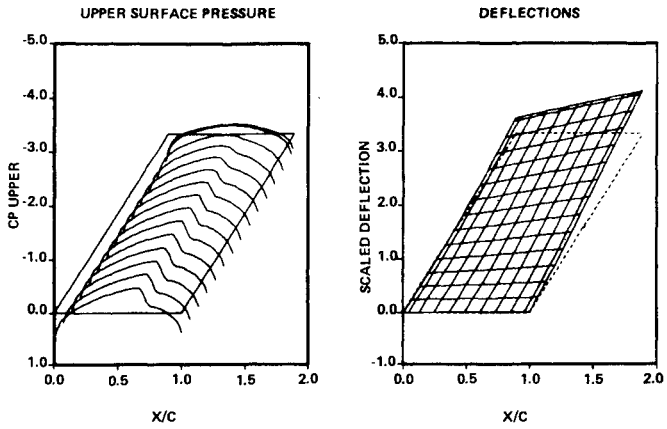

Fig. 4 Pressure distribution and aeroelastic deflection for rectangular wing at $M_\infty = 0.875$, $Q = 12.15$ kPa (1.75 lb/in.^{2}), $t^* = 1.330$ s.

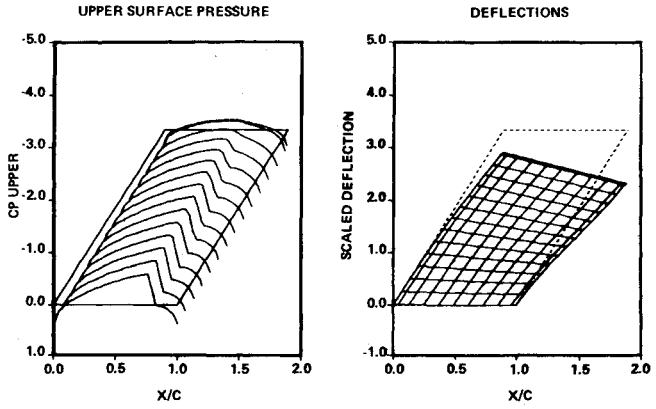

Fig. 5 Pressure distribution and aeroelastic deflection for rectangular wing at $M_\infty = 0.875$, $Q = 12.15$ kPa (1.75 lb/in.^{2}), $t^* = 1.535$ s.

Generalized displacements of all other modes appeared to be well damped for each dynamic pressure. In Fig. 3a, corresponding to a dynamic pressure of 5.21 kPa, the solution covers about five cycles of oscillation of the fundamental mode, and is slightly damped. At 8.68 kPa, as shown in Fig. 3b, the solution is slightly undamped, growing about 10% in amplitude over four cycles of oscillation. In Fig. 3c, the solution for 12.15 kPa is highly undamped, growing to nearly double amplitude in less than four cycles. An extraction of the damping from the time histories by a simple log-decrement method, and interpolation in dynamic pressure, leads to a flutter (neutrally damped) dynamic pressure of approximately 7.29 kPa (1.05 lb/in.^{2}), as shown in Fig. 2. For time histories of the second and higher generalized displacements, a high degree of coupling with the first mode is evident, and the simple log-decrement method is not appropriate for extracting damping. Examination of the results near neutral stability shows the fundamental mode to be most critical for this Mach number range.

Examples of the time-dependent pressures and surface deflections are shown in Figs. 4 and 5. Figure 4 shows the deflected shape and corresponding upper surface pressure coefficient at a point near the maximum upward deflection of the wing during the fourth cycle of oscillation, and Fig. 5 shows a point near the maximum downward deflection. It can be seen that a significant forward motion and weakening of the shock accompanies the upward deflection and consequent "wash out" of the wing, while a rearward motion and strengthening of the shock accompanies the downward deflection. The extent of the shock motion is about 10% of chord. As seen in Fig. 5, the deflected shape during the undamped motion indicates coupling between the bending and torsional modes.

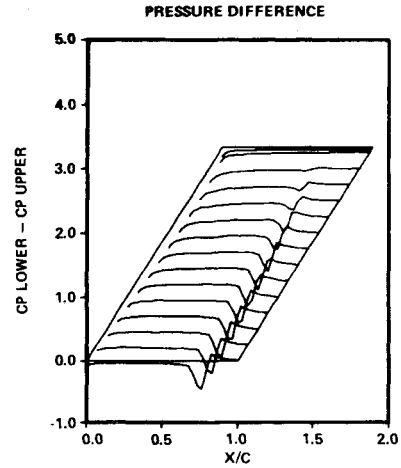

Fig. 6a Pressure difference for rectangular wing at $M_\infty = 0.875$, $Q = 12.15$ kPa (1.75 lb/in.^{2}), $t^* = 1.330$ s.

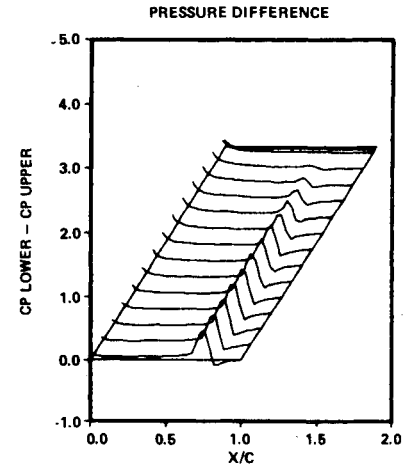

Fig. 6b Pressure difference for rectangular wing at $M_\infty = 0.875$, $Q = 12.15$ kPa, (1.75 lb/in.^{2}), $t^* = 1.535$.

A critical question in transonic flutter analysis has been the character and role of oscillating shocks in the coupled aeroelastic response. Figures 6a and 6b show the pressure difference at the same points in the oscillating cycle as Figs. 4 and 5. It may be seen in this case that most of the aerodynamic loading during the cycle of oscillation is due to the presence and motion of the shocks on the upper and lower surfaces, as shown by the width and magnitude of the "pressure pulse" occurring on the aft section of the airfoil. It may also be seen that there are significant three-dimensional effects in the pressure difference.

VI. Conclusions and Discussion

A numerical method for calculating the three-dimensional unsteady pressure distributions on wings undergoing general time-dependent motion in transonic flow, and for performing coupled aeroelastic calculations, has been developed. The method has been incorporated in a procedure for determining the transonic flutter boundary (i.e., dynamic pressure at flutter as a function of Mach number) for a wing with a given aerodynamic configuration, structural definition, and inertial properties. The method can be used with simple (beam-like) or complex (finite element) structural definitions. The method produces "matched-point" solutions, and is capable of

predicting damped, neutrally damped, or undamped (dynamically unstable) aeroelastic response.

The method has been demonstrated by performing a coupled aeroelastic analysis on a simple rectangular wing at several Mach numbers and dynamic pressures. The validity of the procedure has been shown by comparison with several other flutter prediction methods, including the doublet lattice method, modified strip theory, and a time-linearized transonic method. The nonlinear time integration method has exhibited several unique capabilities, however, including the significant interaction between the unsteady shock motions and dynamic motion of the elastic wing, and the existence of the "transonic bucket" without the necessity for empirical corrections.

Much additional work could be performed in continued development and application of the present method. A comprehensive study of the effects of both static and dynamic initial conditions (e.g., angle of attack, modal deflection) should be undertaken. The important contribution of viscous effects, including shock/boundary-layer interaction, boundary-layer displacement effects, and separation to aeroelastic stability and response should be investigated. This may be accomplished by modification of the surface boundary conditions in a coupled, time-dependent fashion. More complex and realistic wing configurations, including the effects of sweep, taper, and advanced airfoil sections may be treated with the present method, and extensions to include pylon-nacelle-store, and empennage, winglet, and fuselage interference effects are possible. Applications to other aeroelastic problems, including static divergence, dynamic loading, gust response, and active control effects should be studied. Finally, the method requires a more thorough validation than the preliminary results presented here. A comprehensive comparison with experimental data for a variety of configurations, in order to establish the range of applicability of the unsteady modified small disturbance method, is needed.

Acknowledgments

This work was partially sponsored by the U.S. Air Force under Contract F33615-78-C-3201. The authors would like to acknowledge the contributions of several co-workers, including D. W. Gimmestad, who assisted with the modified strip theory analysis and A. J. Christiansen who provided the doublet lattice results. Use of the CDC 7600 at NASA Ames Research Center, was provided through the auspices of the Applied Computational Aerodynamics Branch.

References

[1] Murman, E. M. and Cole, J. D., "Calculation of Plane Steady Transonic Flows," *AIAA Journal*, Vol. 9, Jan. 1971, pp. 114-121.

[2] Magnus, R. J. and Yoshihara, H., "Inviscid Transonic Flow Over Airfoils," AIAA Paper 70-47, Jan. 1970.

[3] Magnus, R. H. and Yoshihara, H., "Unsteady Transonic Flows Over an Airfoil," *AIAA Journal*, Vol. 13, Dec. 1975, pp. 1622-1628.

[4] Ballhaus, W. F. and Bailey, F. R., "Numerical Calculation of Transonic Flow About Swept Wings," AIAA Paper 72-677, June 1972.

[5] Mason, W., Mackenzie, D. A., Stern, M. A., and Johnson, J. D., "A Numerical Three-Dimensional Viscous Transonic Wing-Body Analysis and Design Tool," AIAA Paper 78-10, Jan. 1978.

[6] Boppe, C. W. and Stern, M. A., "Simulated Transonic Flows for Aircraft with Nacelles, Pylons, and Winglets," AIAA Paper 80-104, Jan. 1980.

[7] Jameson, A. and Caughey, D. A., "A Finite Volume Method for Transonic Potential Flow Calculations," AIAA Paper 77-635, June 1977.

[8] Holst, T. L., "A Fast, Conservative Algorithm for Solving the Transonic Full-Potential Equation," AIAA Paper 79-1456, July 1979.

[9] Traci, R. M., Albano, E. D., and Farr, J. L., "Small Disturbance Transonic Flows About Oscillating Airfoils," AFFDL-TR-74-37, June 1974.

[10] Ehlers, F. E., "A Finite Difference Method for the Solution of the Transonic Flow Around Harmonically Oscillating Wings," AIAA Paper 74-543, June 1974.

[11] Weatherill, W. H., Ehlers, R. E., and Sebastian, J. D., "Computation of the Transonic Perturbation Flow Field Around Two- and Three-Dimensional Oscillating Wings," AIAA Paper 76-99, Jan. 1976.

[12] Traci, R. M., Albano, E. D., and Farr, J. L., "Small Disturbance Transonic Flows About Oscillating Airfoils and Planar Wings," AFFDL-TR-100, Aug. 1975.

[13] Seebass, A. R., Yu, N. J., and Fung, K. Y., "Unsteady Transonic Flow Computations," *Unsteady Aerodynamics*, AGARD CP-227, Sept. 1977, pp. 11-1 to 11-17.

[14] Ballhuas, W. H. and Goorjian, P. M., "Implicit Finite-Difference Computations of Unsteady Transonic Flows About Airfoils," *AIAA Journal*, Vol. 15, Dec. 1977, pp. 1728-1735.

[15] Chin, W. C., "Harmonic Analysis of Unsteady Transonic Flow," *AIAA Journal*, Vol. 19, Feb. 1981, pp. 236-237.

[16] Tijdeman, H., "Investigation of the Transonic Flow Around Oscillating Airfoils," NLR Rept. TR 77090, The Netherlands, Dec. 1977.

[17] Weatherill, W. H. and Ehlers, F. E., "Analysis of Transonic Flow About Harmonically Oscillating Airfoils and Wings," AIAA Paper 80-0149, Jan. 1980.

[18] Ashley, H., "Role of Shocks in the Sub-Transonic Flutter Phenomenon," *Journal of Aircraft*, Vol. 17, March 1980, pp. 187-197.

[19] Rizzetta, D. P. and Chin, W. C., "Effect of Frequency in Unsteady Transonic Flow," *AIAA Journal*, Vol. 17, July 1979, pp. 779-781.

[20] Ballhaus, W. F. and Goorjian, P. M., "Computation of Unsteady Transonic Flows by the Indicial Method," *AIAA Journal*, Vol. 16, Feb. 1978, pp. 117-124.

[21] Yang, T. Y., Guruswamy, P., and Striz, A. G., "Aeroelastic Response Analysis of Two Dimensional, Single and Two Degree of Freedom Airfoils in Low-Frequency, Small Disturbance Unsteady Transonic Flow," AFFDL-TR-79-3077, June 1979.

[22] Rizzetta, D. P., "Time Dependent Response of a Two-Dimensional Airfoil in Transonic Flow," *AIAA Journal*, Vol. 17, Jan. 1979, pp. 26-32.

[23] Steger, J. L. and Bailey, H. E., "Calculation of Transonic Aileron Buzz," AIAA Paper 79-0137, Jan. 1979.

[24] Borland, C. J., Rizzetta, D. P., and Yoshihara, H., "Numerical Solution of Three-Dimensional Unsteady Transonic Flow Over Swept Wings," *AIAA Journal*, Vol. 20, March 1982, pp. 340-347.

[25] Lomax, H., Bailey, F. R., and Ballhaus, W. F., "On the Numerical Simulation of Three-Dimensional Transonic Flow with Application to the C-141 Wing," NASA TN D-6933, Aug. 1973.

[26] Ballhaus, W. F., Bailey, F. R., and Frick, J., "Improved Computational Treatment of Transonic Flow About Swept Wings," *Advances in Engineering Science*, Vol. 4, Nov. 1976, pp. 1311-1320.

[27] VanDerVooren, J., Sloof, J. W., Hizing, G. H., and Van Essen, A., "Remarks on the Suitability of Various Transonic Perturbation Equations to Describe Three-Dimensional Transonic Flow-Examples of Computations Using a Fully-Conservative Rotated Difference Scheme," *Symposium Transsonicum II*, Springer-Verlag, Berlin, 1976, pp. 556-557.

[28] Kwak, D., "Non-Reflecting Far Field Boundary Conditions for Unsteady Transonic Flow Computations," AIAA Paper 80-1393, July 1980.

[29] Yoshihara, H., "Formulation of the Three-Dimensional Transonic Unsteady Aerodynamic Problem," AFFDL TR-79-3030, Feb. 1979.

[30] Borland, C. J. and Rizzetta, D. P., "Transonic Unsteady Aerodynamics for Aeroelastic Applications—Vol. I: Technical Development Summary," AFWAL TR-80-3107, Vol. I, June, 1982.

[31] Loring, S. J., "General Approach to the Flutter Problem," *SAE Transactions*, Vol. 49, No. 2, Aug. 1941, pp. 345-356.

[32] Bisplinghoff, R. L., Ashley, H., and Halfman, R. L., *Aeroelasticity*, Addison-Wesley, Cambridge, 1955.

[33] Schwanz, R. C., "Equations of Motion Appropriate to the Analysis of Control Configured Vehicles," AIAA Paper 72-952, Sept. 1972.

[34] Miller, R. D., Kroll, R. I., and Clemmons, R. E., "Dynamic Loads Analysis System (DYLOFLEX) Summary," NASA CR-2846, May 1978.

[35] Smilg, B. and Wasserman, L. S., "Application of Three-Dimensional Flutter Theory to Aircraft Structures," Air Force Tech. Rept. 4798, 1942.

[36] Borland, C. J., Thorne, R. G., and Yeagley, L. R., "Transonic Unsteady Aerodynamics for Aeroelastic Applications—Vol. II: User's Manual," AFWAL-TR-80-3107, Vol. II, June 1982.

[37] Thorne, R. G. and Yeagley, L. R., "Transonic Unsteady Aerodynamics for Aeroelastic Applications—Vol. III: Programmer's Manual," AFWAL-TR-80-3107, Vol. III, June 1982.

[38] Eastep, F. E. and Olsen, J. J., "Transonic Flutter Analysis of a Rectangular Wing with Conventional Airfoil Sections," *AIAA Journal*, Vol. 18, Oct. 1980, pp. 1159-1164.

[39] Bhatia, K. G., "An Automated Method for Determining the Flutter Velocity and the Matched Point," *Journal of Aircraft*, Vol. 11, Jan. 1974, pp. 21-27.

[40] Albano, E. D. and Rodden, W. P., "A Doublet-Lattice Method for Calculating Lift Distribution on Oscillating Surfaces in Subsonic Flows," *AIAA Journal*, Vol. 7, Feb. 1969, pp. 279-285.

[41] Gimmestad, D. W., "A Simplified Flutter Analysis Formulation with Bent Beam Capability," Boeing Document D6-23417TN, Aug. 1968.